

Responses of Trigeminal Ganglion Neurons to the Radial Distance of Contact During Active Vibrissal Touch

Marcin Szwed,* Knarik Bagdasarian,* Barak Blumenfeld, Omri Barak, Dori Derdikman, and Ehud Ahissar

Department of Neurobiology, The Weizmann Institute of Science, Rehovot, Israel

Submitted 1 June 2005; accepted in final form 26 September 2005

Szwed, Marcin, Knarik Bagdasarian, Barak Blumenfeld, Omri Barak, Dori Derdikman, and Ehud Ahissar. Responses of trigeminal ganglion neurons to the radial distance of contact during active vibrissal touch. *J Neurophysiol* 95: 791–802, 2006. First published October 5, 2005; doi:10.1152/jn.00571.2005. Rats explore their environment by actively moving their whiskers. Recently, we described how object location in the horizontal (front–back) axis is encoded by first-order neurons in the trigeminal ganglion (TG) by spike timing. Here we show how TG neurons encode object location along the radial coordinate, i.e., from the snout outward. Using extracellular recordings from urethane-anesthetized rats and electrically induced whisking, we found that TG neurons encode radial distance primarily by the number of spikes fired. When an object was positioned closer to the whisker root, all touch-selective neurons recorded fired more spikes. Some of these cells responded exclusively to objects located near the base of whiskers, signaling proximal touch by an identity (labeled-line) code. A number of tonic touch-selective neurons also decreased delays from touch to the first spike and decreased interspike intervals for closer object positions. Information theory analysis revealed that near-certainty discrimination between two objects separated by 30% of the length of whiskers was possible for some single cells. However, encoding reliability was usually lower as a result of large trial-by-trial response variability. Our current findings, together with the identity coding suggested by anatomy for the vertical dimension and the temporal coding of the horizontal dimension, suggest that object location is encoded by separate neuronal variables along the three spatial dimensions: temporal for the horizontal, spatial for the vertical, and spike rate for the radial dimension.

INTRODUCTION

Whiskers are remarkably efficient sensors (Dehnhardt et al. 2001). Rats rely on their whiskers to estimate the location of objects relative to their heads (Brecht et al. 1997; Carvell and Simons 1990; Hutson and Masterton 1986; Jenkinson and Glickstein 2000; Krupa et al. 2001, 2004; Sachdev et al. 2000; Vincent 1912; Welker 1964). Understanding how the vibrissal system locates objects requires understanding the encoding stage—the responses of first-order neurons, i.e., neurons that receive their input from mechanoreceptors of the whisker follicle–sinus complex (FSC; Ebara 2002; Rice et al. 1986). These neurons, located in the trigeminal ganglion (TG), also referred to as NV) constitute the first stage of the vibrissal system (Tracey and Waite 1995).

Muscle-driven, whiskinglike movements (artificial whisking; Brown and Waite 1974; Semba and Egger 1986; Szwed et al. 2003; Zucker and Welker 1969) that have trajectories similar to natural whisking (Szwed et al. 2003) can be induced

by applying electrical stimuli to the facial motor nerve (Fig. 1A). With artificial whisking, it is possible to record responses to ecologically relevant stimuli under controlled conditions impossible to achieve with behaving animals (Arabzadeh et al. 2005; Nguyen and Kleinfeld 2005). During artificial whisking, like during self-evoked whisking, the whisker is actively pulled by intrinsic muscles (Fig. 1B). In contrast, passive stimuli achieved by deflecting stationary whiskers or when the rat moves near objects without whisking act only on the external shaft of the whisker (Fig. 1C). Forces that act on receptors in the whisker follicle during artificial whisking, and consequently the types of neural responses observed, are different from the types of responses to passive deflection stimuli (Szwed et al. 2003).

Previously, our analysis of the responses of TG neurons during artificial whisking revealed that they can be divided into three main categories (Szwed et al. 2003): “Whisking cells,” which respond only to whisking; “Whisking/Touch cells,” which respond both to touch and whisking; and “Touch cells,” which respond to touch only (Table 1). Touch neurons can be further divided into “Contact,” “Detach,” and “Pressure” subpopulations, which are active at different phases of the whisking cycle. “Contact” Touch cells fire short phasic bursts when the whisker touches an object, whereas “Detach” Touch cells fire short phasic bursts when the whisker starts to retract and detach from the object. “Pressure” Touch cells fire long tonic bursts that last as long as the whisker is pressing against the object.

The dimensions of whisker-related spatial coordinates are: vertical (parallel to whisker arcs; typically vertical to the ground), horizontal (parallel to whisker rows), and radial (along a whisker, from the snout out; Fig. 1, *D* and *E*). Recently, we demonstrated that the horizontal coordinate of object location, i.e., its position on the front–back axis, is encoded in two ways that are based on response timing: by the temporal interval between the onset firing of Whisking cells and that of Contact cells, and by the identity of the Whisking cells that fire synchronously with Contact cells (Szwed et al. 2003). Herein, we examined the encoding of another coordinate—the radial distance of object location. Our questions were: how various TG cell populations encode the radial dimension of object location, what are the neuronal variables used, and how much information is conveyed by single neurons and by cell populations.

* M. Szwed and K. Bagdasarian contributed equally to this work.

Address for reprint requests and other correspondence: Ehud Ahissar, Department of Neurobiology, The Weizmann Institute of Science, Rehovot 76100, Israel (Email: ehud.ahissar@weizmann.ac.il).

The costs of publication of this article were defrayed in part by the payment of page charges. The article must therefore be hereby marked “advertisement” in accordance with 18 U.S.C. Section 1734 solely to indicate this fact.

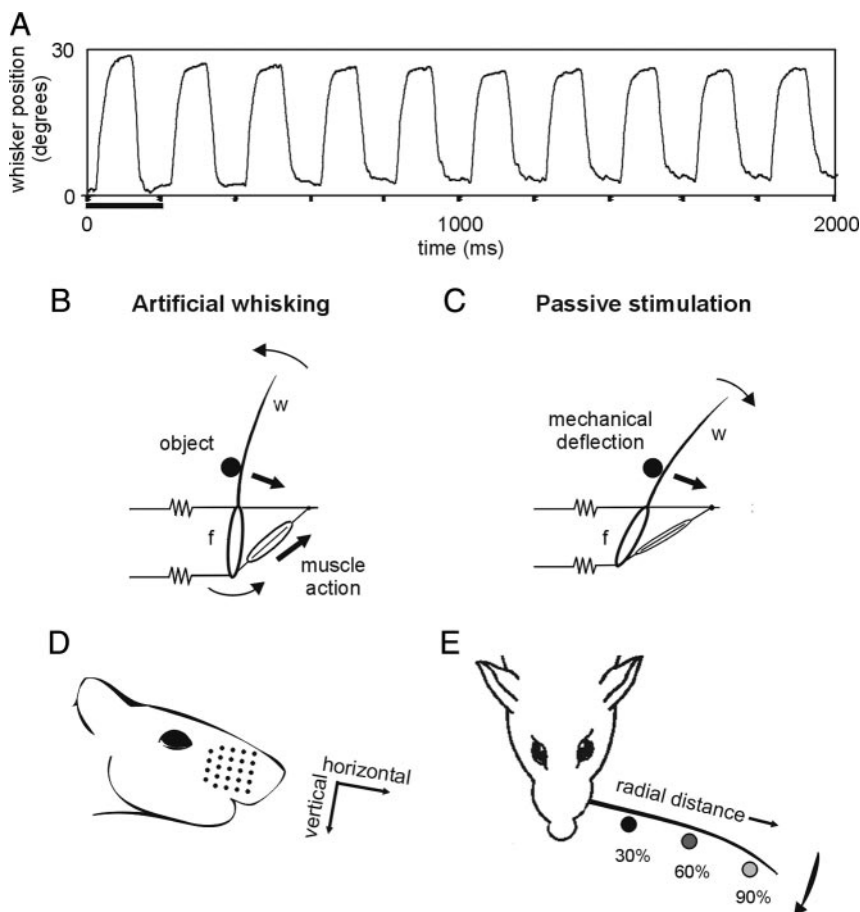


FIG. 1. Artificial whisking and experimental paradigm. *A*: Whisker trajectory during free-air artificial whisking at 5 Hz. Thick horizontal bar denotes one whisking cycle. *B* and *C*: depiction of forces acting on the whisker–follicle complex by the intrinsic muscle and the external object during artificial whisking, *B*, and passive deflection, *C*: *w*, whisker; *f*, follicle; thick arrows denote forces, thin arrows directions of movement. Forces applied by the extrinsic muscles are not depicted. *D*: Whisker-related spatial coordinates: vertical (parallel to whisker arcs), horizontal (parallel to whisker rows), and radial (along a whisker); *E*: experimental paradigm. Rat is artificially whisking at 5 Hz in free air, and against an object (circles) located at 90% (distal), 60%, and 30% (proximal) of the length of the whisker measured from the base. Whisker movements are captured by a fast digital video camera. Curved arrow shows the direction of whisking. *B* and *C* adapted with permission from Berg and Kleinfeld (2003).

METHODS

Animal preparations and electrophysiology

Anesthetized (urethane, 1.5 g/kg, administered intraperitoneally) male Albino Wistar rats (200–300 g, $n = 45$) were secured in a stereotaxic device (SR-6; Narishige, Tokyo, Japan) and placed on a servo-controlled heating blanket. Supplemental doses of anesthesia (10%) were administered when required, and atropine methyl nitrate (0.3 mg/kg, administered intramuscularly) was administered to prevent respiratory complication. During surgery and experimental manipulations, body temperature was maintained at 37°C, and monitored rectally. An opening was made in the skull overlying the left TG, and glass-coated tungsten microelectrodes (0.5–1 M Ω , Alpha Omega Engineering, Nazareth Illit, Israel) were lowered to the ganglion at stereotaxic coordinates previously described (Schneider et al. 1981;

Shoykhet et al. 2000) until units drivable by manual whisker stimulations were encountered. All protocols involving the experimental animals were conducted in accordance with National Institutes of Health regulations and approved in advance by the Animal Care Committee of the Weizmann Institute of Science. Standard methods for single-unit recordings were used (Sosnik et al. 2001). Artifacts produced by electrical stimulation were isolated by a spike-sorter (MSD-3.21; Alpha Omega Engineering) and removed from unit recordings (see Szwed et al. 2003 for discussion). Other sources of recordings were precluded by the anatomic location of the ganglion (Schneider et al. 1981) and the highly typical responses of primary afferent cells (Shoykhet et al. 2000; Zucker and Welker 1969).

Artificial whisking and experimental paradigms

Artificial whisking was induced by stimulating the buccal motor branch of the facial nerve (Semba and Egger 1986; Szwed et al. 2003). The facial nerve was exposed and cut, its distal end mounted on bipolar silver electrodes, and the nerve was kept moist by frequent brief washes with warm saline between periods of stimulation. Bipolar rectangle electrical pulses were applied [0.5–4.0 V, 83 Hz, 40- μ s duration; parameters adapted from Brown and Waite (1974)] through an isolated pulse stimulator (2 \times ISO-Flex; A.M.P.I., Jerusalem, Israel). In each experiment, the stimulus voltage was adjusted to produce maximum movement amplitude. These parameters (stimulus voltage and movement velocity) evoked full-field whisker movement patterns similar to those observed during natural whisking (Szwed et al. 2003). When whisker movement velocity was manipulated, 50% velocity was obtained by decreasing the voltage of stimulation pulses.

It must be noted that some differences exist between our experimental conditions and natural ones, which probably affect the me-

TABLE 1. Responses of TG neurons during active touch

Whisking	Touch	Whisking/ Touch
Respond to whisking only	Respond only to touch	Respond both to whisking and touch
		Pressure
		Contact + Detach
		Fire continuously as long as whisker presses at object
		Fire briefly when whisker touches and/or detaches from object

chanics of whisker movement and interactions with the environment. In awake whisking animals, sympathetic and parasympathetic activation monitor blood supply to the follicle (Fundin et al. 1997), which besides possibly affecting geometrical movement parameters of the follicle, might also affect the sensitivity of its mechanoreceptors (Gottschaldt et al. 1973). Whether similar effects occur during electrical stimulation of the facial nerve is not yet known. In awake animals, whisker retraction involves activation of extrinsic facial muscles (Berg and Kleinfeld 2003). In our artificial paradigm, both intrinsic and extrinsic muscles are activated during protraction, whereas retraction is passive. With artificial whisking, a small stimulus-locked component (83 Hz in our case) is superimposed on the main protraction trajectory (Szwed et al. 2003). Although the basics of muscle-driven whisker movement and of the pattern of movement trajectory were preserved in our experiments, the details of movements and mechanical interactions probably differ somewhat from those that naturally occur.

Artificial whisking was induced by 5 Hz (50% duty cycle) trains for 2 s followed by 2-s intertrain intervals in blocks of 12 trains (trials). Blocks of free-air artificial whisking were interleaved with similar blocks of artificial whisking against a prepositioned object. The object, a vertical steel rod (diameter 1.8 mm) was mounted in a micromanipulator (SM-25B, Narishige) and positioned in front of resting whisker, at 30, 60, and 90% of the whisker's length (measured from its emergence from the skin surface to its tip). At each of these radial distances, the obstacle was positioned at the same angle with respect to the resting whisker; as a result, the duration of touch was the same for all three object positions. Whisker movements were recorded at 1,000 frames per second (fps) with a fast digital video camera (MotionScope PCI 1000; Redlake, San Diego, CA). Recording was synchronized with neurophysiological data with 1-ms accuracy through a TTL signal from the data-acquisition computer.

Data analysis

Trajectories of whisker movements and whisker mechanics were analyzed off-line, using a semiautomated whisker-tracking system (Knutsen et al. 2005). Movement amplitude was defined as the difference between the angles of the whiskers in the resting and most protracted (end of muscle contraction, 100 ms after stimulus onset) positions. Whisker-object contact times could be determined with 2-ms precision. Statistical analysis was done in MINITAB (Minitab; State College, PA), Excel and MATLAB (The MathWorks, Natick, MA). All data were tested for normality. Nonnormally distributed data ($P < 0.05$; Kolmogorov–Smirnov) was subjected to nonparametric tests (Mann–Whitney or Kruskal–Wallis). Mixed normal and nonnormal samples (such as delays to the first spike) were subjected to ANOVA and then nonparametric tests (Mann–Whitney or Kruskal–Wallis) to validate their results. When multiple tests were applied to a sample, the lower P value was chosen.

Complexity was reduced by treating Contact cells ($n = 9$), Detach cells ($n = 4$), and Contact/Detach cells ($n = 3$) as one group referred to as “Contact + Detach” cells. After recording 28 Touch cells and 15 Whisking/Touch cells, we decided to record Touch cells only; subsequently encountered Whisking/Touch cells were ignored and additional Touch cells ($n = 10$) were recorded. Some (23/53) of the TG cells used in this study were also used in our study on coding of horizontal object location (Szwed et al. 2003).

ISIs were calculated for responses within one whisking cycle for cells that fired more than two spikes per trial. Response duration was estimated from peristimulus time histograms (PSTHs) computed for all trials with 1-ms bins, smoothed by convolution with a triangle of area 1 and a base of ± 10 ms. Delay to first spike was measured from the moment of whisker-object contact (as determined by the video data). For cells in which differences between mean delays for the three object positions were < 2 ms (the contact estimation error) no encoding by delay to first spike was assumed.

We estimated mutual information (MI) (Shannon 1948) between the different stimuli (30, 60, and 90%; henceforth denoted as S) and the responses (spike count, delay to first spike, ISI, and populations; henceforth denoted as R). MI quantifies the reduction in uncertainty (entropy) about a stimulus, given the response

$$I(S; R) = \sum_s P(s) \sum_r P(r|s) \log_2 \frac{P(r|s)}{P(r)}$$

Because there were only 120 experimental trials per condition, an estimator of the MI was used and the bias resulting from the estimation corrected, as described by Panzeri and Treves (1996). MI modeling was implemented in MATLAB using histogram2.m by R. Moddemeijer and bayescount.m by S. Panzeri (available at <http://www.cs.rug.nl/~rudy/matlab/doc/histogram2.html>, <http://personalpages.umist.ac.uk/staff/S.Panzeri/software.htm>). All variables were binned into 1-ms bins. For whiskers with three or more spikes (and thus more than one ISI value), the average ISI values within the cycle were used to calculate the MI content for the ISI code.

Receiver-operator characteristic (ROC) curves for pairs of stimuli (30 vs. 60% or 60 vs. 90%) were generated using distributions of the neuronal response variables in the two conditions. These distributions were denoted by $P(r_1)$, $P(r_2)$, with r_1 selected to be the response that typically takes smaller values. ROC curves were plotted by fixing a threshold T , and calculating $P(r_1 > T)$ against $P(r_2 > T)$. The entire ROC curve was plotted by varying T over the entire range of values achieved by the neuronal response. The area under the ROC curve was calculated using the trapezoidal integration rule. This method is equivalent to calculating the probability $P(r_1 > r_2) + P(r_1 = r_2)/2$.

For both ROC and MI population analysis, a weighted sum of the individual responses was used to create a higher-order discriminator. Negative weights were allowed because inhibitory connections are abundant in the next station of the trigeminal system, the brain stem (Jacquin et al. 1989; Lo et al. 1999). Because neurons were recorded one at a time, the correlation between their responses could not be assessed. For our analysis we assumed uncorrelated responses.

Both population MIs and ROC curves of neuronal ensembles were generated by first constructing pseudosimultaneous response vectors by randomly mixing responses of different units, after which dimensionality of the vectors was reduced using linear discriminant analysis (LDA), which provides a robust and straightforward method of reducing dimensionality (Morrison 1976). For the MI, dimensionality was reduced to 2. For the ROC, the LDA algorithm was used to separate the response for the two stimulus values for which ROC curve was constructed, and the dimensionality was reduced to 1. In the latter case, the LDA algorithm reduces to assigning each neuron a weight proportional to: $(\mu_1 - \mu_2)/(\sigma_1^2 + \sigma_2^2)$, with μ_j , σ_j^2 denoting the mean and variance of the response to the j th stimulus, respectively.

RESULTS

Artificial whisking and the experimental paradigm

We induced artificial whisking in urethane-anesthetized rats by stimulating the facial motor nerve. Extracellular recordings were obtained from 53 TG neurons during artificial whisking at 5 Hz. TG cells exhibited little or no spontaneous activity (average 0.06 spikes/s). All neurons had single-whisker receptive fields (as previously reported by Gibson and Welker 1983b; Lichtenstein et al. 1990; Shoykhet et al. 2000; Szwed et al. 2003; Zucker and Welker 1969). We recorded units that had receptive fields on large whiskers from rows B to E and straddler to 4th arcs. Whisker trajectories in the horizontal plane (Fig. 1A) were captured with a fast digital video camera (1,000 fps) synchronized with the neural data-acquisition computer. Because of space and illumination constraints, neurons

that had receptive fields on row A were not recorded. Video data were analyzed with a semiautomated whisker-tracking system (Knutsen et al. 2005).

Figure 1E shows our experimental design. Blocks of whisking in free air were interleaved with blocks of whisking against an object (vertical pole) located in three different radial positions: 90% (distal), 60%, and 30% (proximal) of whisker length measured from the snout of the rat (see Fig. 1E). All neurons were recorded one at a time. The amplitude of movement varied from one experiment to another as a result of variations in electrode-nerve coupling and nerve condition. The variability was $\pm 5.7^\circ$ (SD; $n = 53$) from the mean amplitude of 18.2° . Movement angular velocities, measured in the early part of the protraction phase (5 to 20 ms after movement onset), were 420 ± 123 deg/s (mean \pm SD; $n = 38$ Touch cells). Such velocities and amplitudes are within the lower range of whisking velocities and amplitudes observed in rats during texture discrimination (see Fig. 5 in Carvell and Simons 1990) and free exploration (P. Knutsen, M. Pietr, and E. Ahissar, unpublished observations). Retraction velocities were 705 ± 223 deg/sec; the protraction/retraction ratios in our experiments were thus similar to those observed during self-evoked whisking (Bermejo et al. 2002; Carvell and Simons 1990; P. Knutsen, et al., unpublished observations). In all cases analyzed ($n = 38$), retraction velocity was higher than protraction velocity. Movement amplitude and protraction velocity were tightly correlated ($R^2 = 0.74$, $P < 0.001$).

Responses of TG cells are influenced by the horizontal coordinate of touch, i.e., by the horizontal angle of the whisker at the time of touch (Szwed et al. 2003) and by stimulus velocity (Arabzadeh et al. 2005; Gibson and Welker 1983b; Jones et al. 2004a,b; Lichtenstein et al. 1990; Shoykhet et al. 2000; Zucker and Welker 1969). To eliminate these influences

and measure exclusively the effect of radial object position, we used the same movement velocity and angular position of the object (with respect to resting whisker) for all three radial positions. The object was carefully positioned with a micro-manipulator and post hoc analysis of whisker movements was used to exclude cells for which either the velocity of the whisker at the moment of touch or angular position of the object differed by more than 15% for the three radial positions. As a result, whisker-object contact durations were identical for all object positions ($P = 0.35$, ANOVA).

Neurons that responded to object touch were divided into two categories as previously described (Table 1 and Szwed et al. 2003): “Touch cells” ($n = 38$), which responded only when the whisker touched the object, and “Whisking/Touch cells” ($n = 15$), which responded both to whisking and to touch. We classified cells as “Whisking/Touch cells” if during whisking in free air they fired more than one spike per five whisks.

Encoding of radial object location by spike count

We first investigated how radial object location is reflected in spike counts of Touch cells. Figure 2A depicts mean spike rates of Touch cells normalized to maximum. Touch cells fired more spikes when the object was closer to the base of the whiskers ($P < 0.001$, ANOVA). Contributions of individual cells to this mean increase in spike count were determined by performing ANOVA on firing rate responses of individual cells to object position with Fisher’s pairwise comparisons at $\alpha = 0.05$. All the Touch cells examined changed their firing rates in response to radial object location ($P < 0.001$ for 31 cells and $P < 0.05$ for the other seven cells). Many Touch cells (15/38, 39%) significantly increased their firing rates both from the 90 to 60% and from the 60 to 30% positions. Slightly more (18/38,

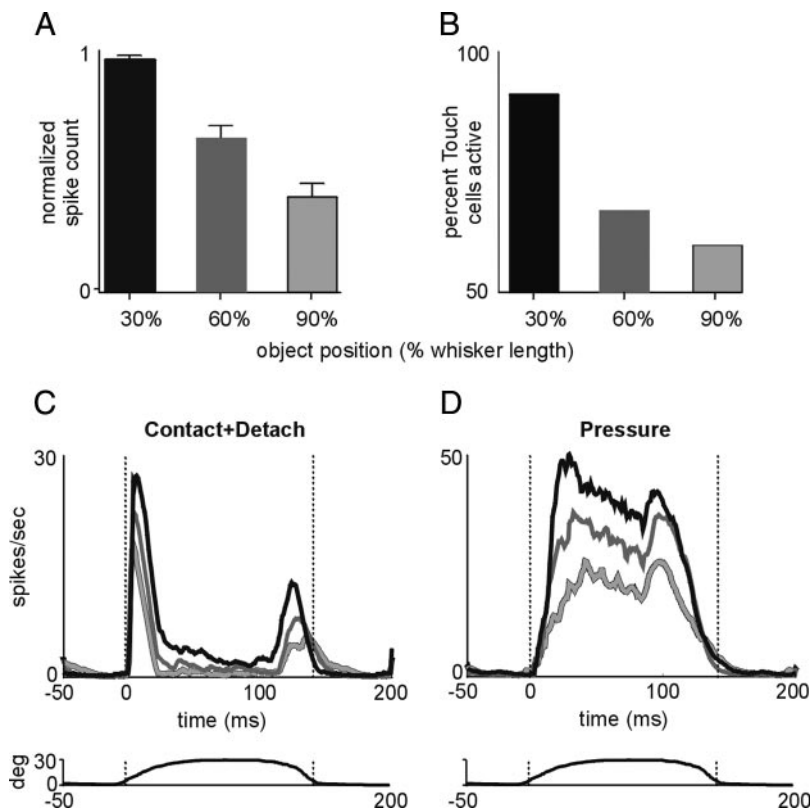


FIG. 2. Encoding of radial object position by Touch cells. *A*: mean spike counts per position of Touch cells ($n = 38$). Bars denote SE. *B*: percentages of Touch cells activated at each of the 3 object positions. *C* and *D*: population peristimulus time histograms (PSTHs) of the Contact + Detach ($n = 16$; *C*) and Pressure ($n = 22$; *D*) Touch cell subtypes, during whisking at objects located at 90% (outlined light gray line), 60% (dark gray line), and 30% (black line) of the whisker length. Graphs below the PSTHs depict a typical free-air trajectory of a single whisker measured at the base of the whisker. All PSTHs were triggered on whisker-object contact and averaged over all trials. Spike counts in *A* were normalized to maximum. Dotted vertical lines in *C* and *D* denote average time of contact and detachment from the object. Whisker-object contact durations were similar for all 3 object positions ($P = 0.35$, ANOVA).

47%) Touch cells significantly increased their firing rates for only one of the two position pairs. The remaining Touch cells (5/38, 13%) increased their firing rate for one of the position pairs, while decreasing the firing rate for the other pair; however, their firing rate at the 30% (proximal) distance was greater than the firing rate at the 90% (distal) distance. We conclude that all Touch neurons fired more spike counts for closer objects.

Encoding of radial object location by number of activated cells

Proximal stimuli also activated more Touch cells than distal stimuli (Fig. 2*B*). In our previous work (Szwed et al. 2003) we reported that 26% of TG cells had high response thresholds, i.e., did not respond to free whisking in air nor to whisking against an object located in the most distal (90%) position, but only to manual stimulation. In the current study, 17 cells had such high response thresholds and fired <1 spike per five whisks when the object was located at 90% of whisker length. Thirteen of these cells started responding when the object was located closer to the snout, at 60 or 30% of whisker length. Four remaining cells did not respond during any of the standard conditions of our paradigm. (They were included in Fig. 2*B* but not analyzed further; interestingly, two of these cells did respond during retraction when an object was placed behind the whisker at a radial distance of 30%; data not shown.)

The response of more cells in more proximal object positions (Fig. 2*B*) was independent of the threshold criterion chosen (one spike per five whisks); for all activity thresholds between 0 and 1 spike/whisk, more cells responded in more proximal object positions. Response thresholds did not depend on touch velocity; whisker velocities at the time of touch did not differ for high-threshold and low-threshold Touch cells ($P = 0.14$, *t*-test). Thus the radial stimuli revealed a potential role for cells with high response thresholds, which fired exclusively when the object was sufficiently proximal. Such behavior might be interpreted as a form of identity code, where a spike fired by a high-threshold Touch cell indicates the presence of an object close to the snout (see DISCUSSION).

Response dynamics

Touch cells can be subdivided into two subpopulations that become active at different phases of the whisking cycle: Pressure cells and Contact + Detach cells (Table 1, Szwed et al. 2003). Population PSTHs for Contact + Detach cells and Pressure cells are depicted in Fig. 2, *C* and *D*. Figure 3 shows single-cell data as PSTHs (*A–D*), single-cycle raster plots (*E–H*), spike counts per one protraction/retraction whisking cycle (*I–L*), delays to the first spike (*M–P*), and interspike intervals (ISIs, *Q–R*) for two Contact + Detach and two Pressure cells.

For both Contact + Detach and Pressure cells, the increase in spike count for more proximal object position was evident in all phases of the response. Specifically, spike counts of Pressure cells were already significantly different 20 ms after contact (Fig. 2*D*). Pressure cells exhibited 83-Hz modulations in their responses, locked to the electrical stimulation that moved the whiskers (Figs. 2*D* and 3, *C* and *D*); these modulations were caused primarily by velocity modulations in whisker movement (Szwed et al. 2003).

Response variability

Consistent with our previous findings (Szwed et al. 2003), Pressure cells fired more spikes per cycle than Contact + Detach cells ($P = 0.03$, ANOVA). The mean population spike counts with objects positioned at 30, 60, and 90% of whisker length were 4.6, 3.5, and 2.3 spikes/whisk, respectively, for Pressure cells, compared with 1.50, 1.21, and 0.8 spikes/whisk, respectively, for Contact + Detach cells. The spike counts of individual Touch cells differed substantially (see Fig. 3, *I–L*). The pooled SDs for the three object positions (which were not significantly different, $P \geq 0.39$, ANOVA) were 1.82 spikes/whisk for Contact + Detach cells and 3.82 spikes/whisk for Pressure cells. Variations in the velocity of touch from cell to cell (average velocity of touch = 420 ± 123 deg/s, mean \pm SD) could account for at least some of the deviations in spikes/whisk (see *Effect of velocity on spike count of Touch cells*). Other potential sources of variability are directional selectivity and intrinsic response variability [see Figs. 1 and 11 in Gibson and Welker (1983b) and Fig. 3 in Lichtenstein et al. (1990)].

We also observed large trial-to-trial variability in responses of individual neurons (see Fig. 3, *I–L*). The CV values of the spike count responses to single positions ranged from 0.10 to 6.3 (median = 0.59, right-skewed distribution). For 33 Touch cells (using data from this study and Szwed et al. 2003) we determined the source of this large variability by recording both the responses to 5-Hz forward-backward ramp-and-hold mechanical deflections (passive stimuli) and responses to artificial whisking against an object located at 90% of the whisker length (for mechanical stimulation protocols, see Szwed et al. 2003). Responses to artificial whisking had larger CVs than responses to mechanical deflections (mean ratio 1.96, $P < 0.001$, paired *t*-test). This variability is partially attributed to the cycle-by-cycle variability in trajectories of artificial whisking (see Fig. 1*A* and Arabzadeh et al. 2005), which is absent during mechanical deflections. Indeed, the variability of responses within each train of artificial whisking was larger than the variability of responses between the same cycles in different trains (mean $CV_{\text{train}}/CV_{\text{cycle}} = 1.28$, $P < 0.001$, paired *t*-test). Another potential source of variability is the variation in the mechanical response of the whisker.

Effect of velocity on spike count of Touch cells

TG cells respond to increased stimulus velocity by firing more spikes (Arabzadeh et al. 2005; Gibson and Welker 1983a,b; Lichtenstein et al. 1990; Zucker and Welker 1969). To quantify this effect during active touch, we correlated the response of each cell with the velocity at the moment of touch (contact velocity). Generally, higher whisker angular velocity on touch was correlated with higher spike counts for Pressure cells ($R^2 = 0.36, 0.35$, and 0.41 for the 30, 60, and 90% positions, respectively, $P < 0.006$), but not for Contact cells ($R^2 < 0.1$, $P > 0.2$). Responses of Pressure cells ($n = 17$) to contact at 30%, plotted against contact velocity are depicted in Fig. 4*A* (velocities could not be determined for five other Pressure cells because of poor video quality). The modest correlation confirms earlier observations that the firing rates of cells are influenced by factors other than touch velocity, such as directional selectivity and sensitivity of the cells [see Figs.

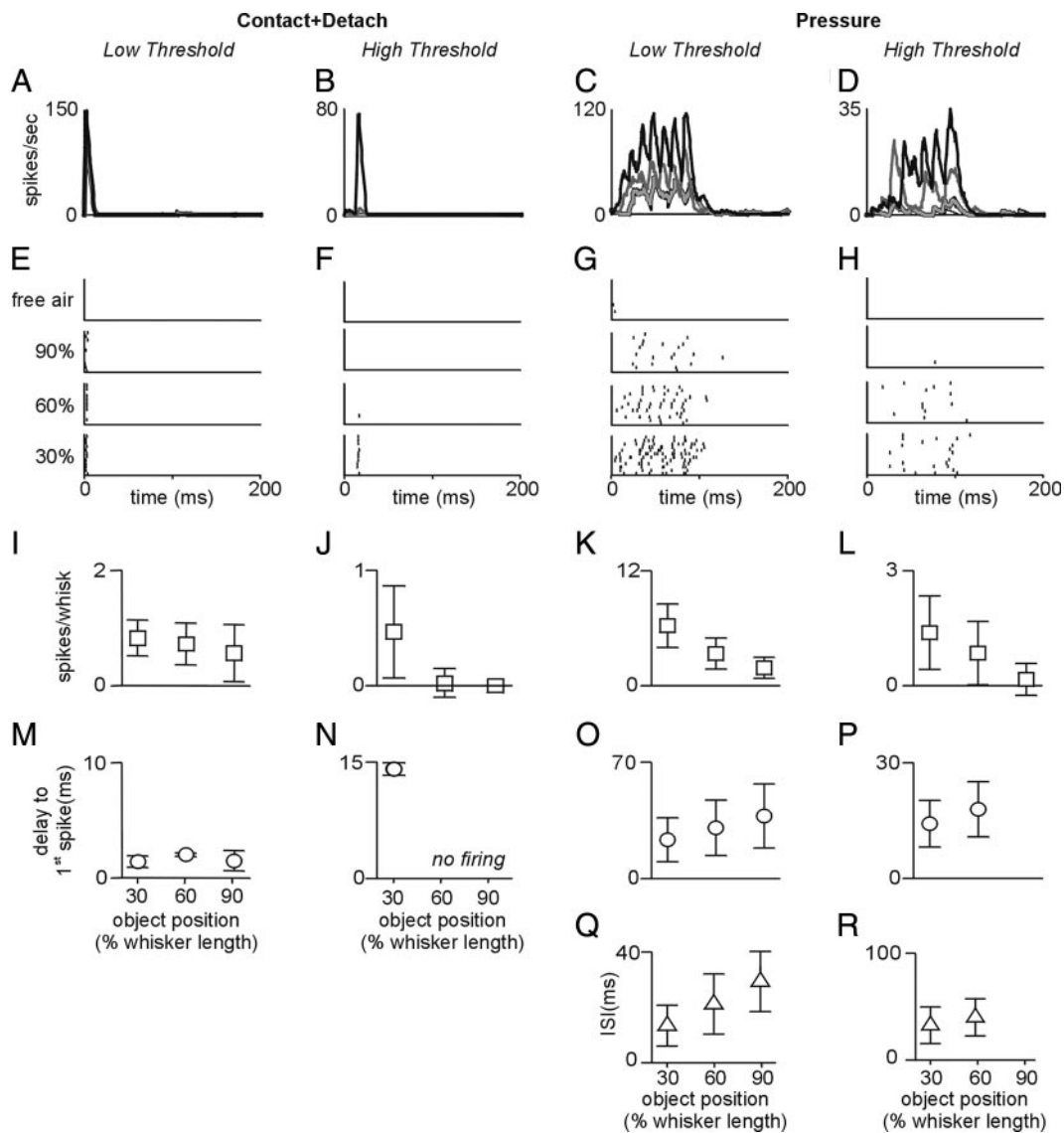


FIG. 3. Encoding of radial object position by individual Contact (2 left columns) and Pressure (2 right columns) Touch cells. Four typical single-cell responses are presented. *A–D*: PSTHs of the responses of individual cells during whisking in free air (dotted line) and at objects located at 90% (distal: light gray line), 60% (dark gray line), and 30% (proximal; black line) of the length of the whiskers; 30 and 60% lines overlay the 90% lines. PSTHs were triggered on whisker–object contact and averaged over all trials. *E–H*: corresponding single-cycle (cycle 3) raster plots. *I–R*: encoding of radial object position by spike counts per cycle (*I–L*), delays to 1st spike (*M–P*), and interspike intervals (ISIs) of Pressure cells (*Q–R*). Variables were averaged for each cell across all trials. Bars denote SD.

1 and 11 in Gibson and Welker (1983b) and Fig. 3 in Lichtenstein et al. (1990)].

To test the effect of contact velocity on responses of individual cells, we recorded the responses of 10 Touch cells (seven Pressure and three Contact + Detach) during whisking at two angular velocities: the maximum velocity obtainable (422 ± 30 deg/s, means \pm SE) and 50% of the maximal velocity. The mean normalized responses of these cells are depicted in Fig. 4*B*. For each of the three radial positions, all 10 cells fired fewer spikes at decreased contact velocity (all $P < 0.001$, *t*-test). When touch velocity was reduced to 50%, spike counts decreased by $54 \pm 7\%$ (means \pm SE; with the magnitude of the decrease being similar for the three positions, $P = 0.86$, ANOVA). Thus both Pressure and Contact + Detach neurons are sensitive to angular velocity on active contact, which is consistent with responses to passive stimuli (Arabza-

deh et al. 2005; Gibson and Welker 1983b; Shoykhet et al. 2000).

We then studied whether the tangential (i.e., linear) velocity of the whisker at contact point correlates with spike rate. Tangential (v) and angular (ω) velocities are linked by the radial distance r ($v = r\omega$). We found that tangential velocity correlates poorly with spike count both at a population level ($R^2 = 0$, $P > 0.34$ for both Pressure and Contact cell populations) and single-cell level (for all 10 cells for which the velocity was varied, the mean R^2 for single-cell regressions was 0.04 ± 0.02 , means \pm SE; all $P > 0.08$). In contrast, single-cell linear correlations of spike count with two predictors—angular velocity (ω) and radial object position (r)—yielded high coefficients of correlation ($R^2 = 0.73 \pm 0.06$, means \pm SE; $P < 0.05$ in eight out of 10 cases). Thus a major part of the spike count responses could be predicted by a linear

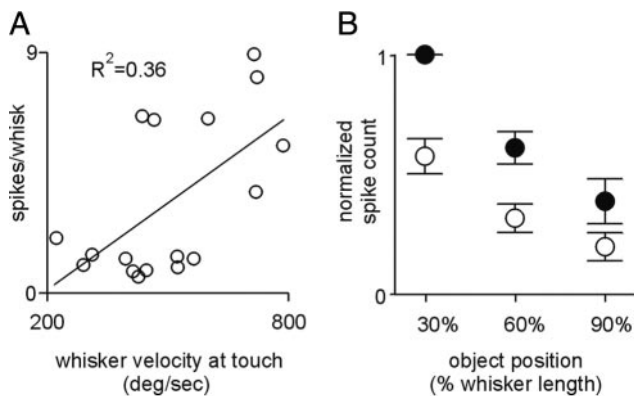


FIG. 4. Effect of whisker velocity at touch on spike count of Touch cells. *A*: influence of the velocity of whisker at the moment of touch on the spike rates of Pressure Touch cells ($R^2 = 0.36$, $P = 0.009$, $n = 17$). Spike rates are shown for objects located at 30% of the whisker length; a similar correlation ($R^2 > 0.34$; $P < 0.006$) was observed for objects located at 60 and 90% of the length (see text). *B*: Touch cells ($n = 10$) were recorded during whisking at full (full circles) and 50% (open circles) contact velocity against objects located at 3 radial distances. Normalized mean firing rates for the 3 object distances are depicted. Bars denote SE.

combination of responses to changes in angular velocity (with positive coefficients) and radial object distance (with negative coefficients).

Encoding by other single-cycle variables

Subsets of Touch cells also responded to radial object position by changes in neuronal variables other than spike count (Fig. 3). Because during tactile discrimination (Carvell and Simons 1990, 1995) and localization (Knutsen et al., unpublished observation) rats appear to use information available in one or a few whisking cycles, we limited our analysis to neuronal variables that are well defined within a single whisking cycle: delay to the first spike and instantaneous firing rate (assessed by the average ISI in a cycle). Herein, the delay to first spike refers to the temporal interval between the time of whisker-object contact and the first spike fired, which is different from the variable encoding the horizontal coordinate of touch (the interval between protraction onset and the first spike fired; Szwed et al. 2003).

Median delays for the object positions of 30, 60, and 90% of whisker length were 10.5, 13.2, and 15.6 ms, respectively, for Pressure cells and 5.1, 5.9, and 5.2 ms, respectively, for Contact + Detach cells. Cells that encoded radial distance by significantly changing their delay to the first spike were detected by the nonparametric Kruskal-Wallis test (delays to the first spike were often distributed nonnormally, Kolmogorov-Smirnov, $P < 0.05$ for 47% of cells). Of the 22 Pressure cells, 17 (77%) encoded the radial position of the object by decreasing the delay between the time of touch and the first spike for more proximal object positions (Table 2). In contrast, only 25% (4/16) of Contact + Detach cells showed a change in delay to the first spike. When the object was at 30% of the whisker length, these four neurons “crossed type,” and started responding with longer delays and tonic bursts similar to Pressure neurons, manifested as an appearance of a tonic component in the population PSTH (Fig. 2*D*, black line). Such behavior was not observed in the remaining 12 nonencoding neurons. [Note, however, that because of the limited temporal

resolution of the video recordings, the existence of temporal coding at a timescale < 2 ms cannot be ruled out for these cells. TG neurons can phase-lock to frequencies $\leq 5,000$ Hz (Gottschaldt and Vahle-Hinz 1981).] Single-cell examples of encoding by delay to first spike are illustrated in Fig. 3, *C*, *D*, *G*, *H*, *O*, and *P*.

Pressure cells also encoded radial object location by decreasing their ISIs. ISIs could be computed only for 13 Pressure cells that fired more than two spikes per cycle in at least two of the three object positions. Mean ISIs for the 30, 60, and 90% of whisker length object positions were 12.7 ± 1.1 , 15.0 ± 1.4 , and 17.5 ± 1.3 ms, respectively (means \pm SE). Of these 13 Pressure cells, 11 (half of the total Pressure cell population) encoded the radial location of the object by decreasing their ISIs for more proximal positions (Table 2; $P < 0.003$ for all significant cells, ANOVA on ISIs of individual cells). The ISIs of the other two cells did not differ across different radial positions ($P > 0.07$, ANOVA).

Encoding efficiency

We assessed the relative encoding efficiencies of the spike count, ISI, and delay codes by performing mutual information (MI, Borst and Theunissen 1999; Panzeri and Schultz 2001; Panzeri and Treves 1996; Shannon 1948) and receiver-operator characteristic (ROC, Britten et al. 1992; Dayan and Abbott 2001; Green 1966) analyses for each of these codes, both at the single-neuron and population levels. In contrast to ANOVA, which provides information about the difference between mean values averaged over the entire 120 trials per position, MI and ROC results can be interpreted as the probability of a correct discrimination based on a single trial. Thus MI and ROC can approximate the real-life performance of a readout circuit that receives information from a particular cell or group of cells.

The amount of information available to the brain by the delay code depends on how the brain extracts it. In the following analysis of the delay code, we assume that the brain uses the temporal information provided by Contact neurons to determine the time of touch (Szwed et al. 2003). More specifically, we assume that the brain decodes the delay between the firing times of Contact + Detach neurons, whose firing timing was not affected by the radial position of the object ($n = 12$ in this study), and those of Pressure neurons. For the brain, this would be the most efficient way to read the temporal information available in its input signals as sampled in this study.

If an outside observer had to guess which of the three possible positions was presented at a given trial, the response of the neurons could be used to reduce the observer’s uncertainty. MI is a measure of that reduction and, as such, it is frequently used to measure the relation between stimulus and

TABLE 2. Percentages of Touch neurons encoding radial position by spike count, delay to first spike, and interspike interval (ISI) variables

Neural Code	Touch Cell Subtype	Encoding Cells, %
Spike count (spikes/whisking cycle)	Pressure ($n = 22$)	100
	Contact + Detach ($n = 16$)	100
Delay to first spike	Pressure ($n = 22$)	77
	Contact + Detach ($n = 16$)	25
ISI	Pressure ($n = 22$)	50

response (Borst and Theunissen 1999; Panzeri and Schultz 2001). MI is measured in bits, which can be intuitively understood as the number of yes/no questions (e.g., is the stimulus applied at 30% of the whisker length?) required to know the stimulus with 100% certainty. In our paradigm, maximum MI is equal to $\log_2(3 \text{ possible values}) = 1.58$ bits of information = 1.58 yes/no questions.

Distributions of MI for individual Pressure and Contact + Detach cells for spike counts, ISIs, and delay codes are depicted in Fig. 5. Pressure cells had higher MI than that of Contact + Detach cells for both spike counts and delay codes ($P < 0.001$, Mann–Whitney). The delay code of Pressure cells had lower MI than the spike-count code ($P = 0.026$, Mann–Whitney). As mentioned previously, Contact + Detach cells did not encode radial object location by delay to the first spike, with the exception of the four “crossed type” cells, which appear as outliers in the *left column* of Fig. 5. For the subset of Pressure cells for which ISI could be computed, the MI content of ISI was similar to the MI of the spike count ($P = 0.24$, $n = 13$, paired t -test).

In addition to the information carried by single neurons we also estimated the amount of information carried by the spike counts, delays, and ISIs of our sample of recorded neurons, assuming uncorrelated responses. For the population of Contact cells ($n = 16$), MI for the spike-count code was 0.82 bit (52%) and for the delay code was 1.33 bits (84%). For the population of Pressure cells ($n = 22$), the spike-count code MI was 1.44 bits (91%), the delay code MI was 1 bit (63%), and the ISI code MI was 0.98 bit (62%).

MI analysis provides an objective assessment of the coding efficiency of various neuronal variables. A complementary, but partially overlapping, question is: what is the efficiency of neuronal circuits in discriminating between specific position pairs. We chose to assess it with ROC analysis, a robust and nonparametric assessment that does not require any assumption about the distributions of the response variables (Britten et al. 1992; Dayan and Abbott 2001; Green 1966). If a behavioral decision in a two-alternative forced-choice task, such as discriminating between two opening sizes (e.g., the task used by

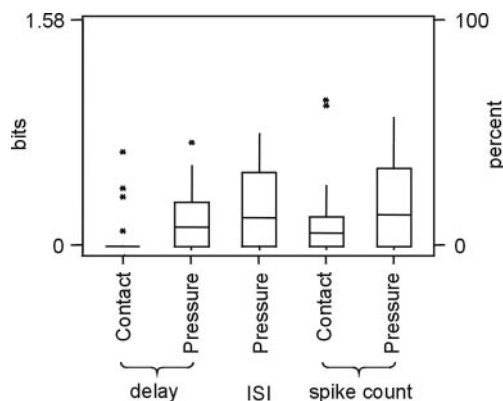


FIG. 5. Comparisons of encoding efficiencies by mutual information (MI). MI for spike count, ISI, and delay to 1st spike codes. Spike count and delay MI contents are plotted separately for Pressure ($n = 22$) and Contact + Detach ($n = 16$) cells. ISI is plotted only for a subset of Pressure cells ($n = 13$) that fired more than 2 spikes per cycle. Distributions of the MIs of individual neurons are indicated by boxes representing the first (25%) to third (75%) quartile values; the lines inside the boxes indicate the medians, and the vertical lines indicate the ranges. Outliers (>3 interquartile values from median) are indicated by stars.

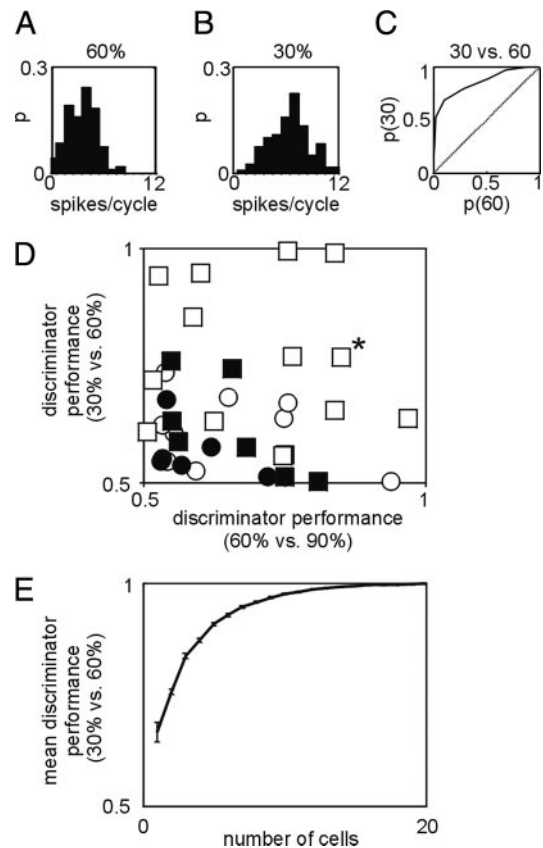


FIG. 6. Receiver-operator characteristic (ROC) assessment of encoding efficiency and dynamics. Spike count histograms for the object positions of 60% (A) and 30% (B) of whisker length for a Pressure cell (Fig. 3, C, G, K, O, and Q). C: ROC curve for the same cell. Probability of correct detection of the 30% stimulus is plotted against the probability of getting a false positive for the same stimulus. Area under the curve represents the probability of making the correct discrimination between the 2 stimuli. Dotted line marks chance level ($P = 0.5$) ROC curve. D: scatterplot of the probabilities of single cells making the correct discrimination between 2 adjacent object positions based on spike count: (○, ●), Contact + Detach cells; (□, ■), Pressure cells. Cells with high response thresholds are depicted by solid symbols. Cell depicted in A–C and in Fig. 3, C, G, K, O, and Q is marked by an asterisk (*). E: mean ROC discriminator performance gradually increases with the size of cell population. Each data point represents average discriminator performance for a subpopulation of n cells randomly chosen from the entire Touch cell population. Bars denote SE.

Krupa et al. 2001), is based on such response variables, the area under the ROC curve would predict the probability of a correct discrimination (Green 1966).

We examined the probability of making the correct discriminations between stimuli at the 30 and 60% positions (30 vs. 60) and between stimuli at the 60 and 90% positions (60 vs. 90) for single cells and for cell ensembles. Two distributions of the spike count responses of a single Pressure neuron, also depicted in Fig. 3, C, G, K, O, and Q, are depicted in Fig. 6, A and B. The resulting ROC curve is shown in Fig. 6C.

The correct discrimination probabilities of all Touch cells for the spike-count code are shown in Fig. 6D, with an asterisk marking the neuron shown in Fig. 3, C, G, K, O, and Q and Fig. 6, A–C. Single cells could support discrimination between two adjacent positions with probabilities as high as 0.99 for spike count (Fig. 6D) and 0.98 for delay and ISI. However, median discrimination probabilities were generally lower: 0.62 for spike count, 0.56 for delay, and 0.63 for ISI. The discrimination probabilities were lower for the delay code than for the

spike-count code (Mann–Whitney, $P = 0.04$), but not significantly different between the ISI and spike-count codes (Mann–Whitney, $P = 0.68$). Cell ensembles could discriminate between two adjacent stimuli with near-perfect accuracy: combined Pressure cells had $P > 0.999$ for spike count, delay, and ISI; combined Contact + Detach cells had $P = 0.993$ for spike count.

We computed how the spike-count–based ROC discrimination capability depends on the size of cell population from which a readout circuit receives input (Fig. 6E) and found that the discriminator performance increased gradually with the number of participating neurons. Average performance of $>95\%$ could be achieved with seven cells randomly chosen from the entire Touch cell population. In the case of high-threshold Touch cells, eight cells were usually needed for $>95\%$ performance. These numbers demonstrate that a relatively small population of uncorrelated neurons is sufficient for obtaining near-certainty discrimination between radial positions 30% of whisker length apart.

Encoding dynamics

Contact + Detach cells have shorter response delays than those of Pressure cells. Contact + Detach cells fire almost all their spikes of the “Contact” response phase within 20 ms of touch, whereas the response durations of Pressure cells are often >100 ms (Fig. 2, C and D). Thus the spike-count code of Contact + Detach cells could be more rapid than that of the Pressure cells. On the other hand, significant differences between responses of Pressure cells to different object positions are visible already at the beginning of their response (see Fig. 2D). We compared fast coding by Contact + Detach and Pressure cells by repeating ROC analysis for all Pressure cells, taking into account only the spike fired in the first 20 ms after touch. Probabilities of a correct discrimination based on the first 20 ms of the response were $92 \pm 15\%$ (average \pm SD) of the probabilities of correct discrimination based on the entire response ($P = 0.001$, paired t -test). Thus most information about radial position is already present in the first 20 ms of the firing of Pressure cells, with additional information being added during the rest of protraction. Despite Contact + Detach cells have earlier firing onsets than Pressure cells (Fig. 2, C and D), in the first 20 ms of response the spikes of these two cell types carry a similar amount of information ($P = 0.68$, t -test). Similar results were obtained using the MI method (not shown).

Encoding by Whisking/Touch cells

All Whisking/Touch cells responded to free-air whisking, but changed their firing patterns when the whisker encountered an object (Fig. 7). The mean spike counts of Whisking/Touch cells were larger on encountering objects than for free-air whisking ($P < 0.001$, ANOVA), but the differences between the mean spike counts for the three radial positions were insignificant ($P = 0.27$, ANOVA). Interestingly, most Whisking/Touch cells (12/15) did vary their spike counts as a function of radial object position ($P < 0.01$, ANOVA). However, these variations were not consistent: seven of the 12 Whisking/Touch neurons fired more spikes for the more distal (60 or 90% of whisker length) position, whereas five fired more spikes for the more proximal (30%) position. Thus the stability of the

mean population rate was not a result of individual Whisking/Touch cells not being affected by the radial object position, but rather because the cells were not affected in a consistent way.

Whisker identity and response parameters

The idea that the large whiskers differ in their mechanics has been a key insight of recent research on the vibrissal system (Hartmann et al. 2003; Neimark et al. 2003). We therefore tested whether there are any significant interrow and interarc differences in neural and response parameters. For rowwise comparisons, straddler whiskers were excluded because they cannot be unequivocally attributed to any row. There was no significant difference between the movement amplitudes for whiskers of different arcs ($P = 0.21$, ANOVA). With respect to rows, whiskers from row E had slightly lower movement amplitudes (mean = 13.5 deg) than those of whiskers from other rows (mean = 20.7; $P = 0.009$, ANOVA with Fisher post hoc comparisons). There were no significant between-row and between-arc differences in evoked spike counts ($P = 0.41$ for rows, $P = 0.22$ for arcs, ANOVA), ROC correct discrimination probabilities ($P = 0.29$ for rows, $P = 0.44$ for arcs, ANOVA), and slopes of spike count tuning curves ($P = 0.28$ for rows, $P = 0.23$, ANOVA). Furthermore, no significant differences were observed for between-row and between-arc distributions of Whisking/Touch compared with Touch cells ($P = 0.50$ for rows, $P = 0.34$ for arcs, Mann–Whitney), high-threshold compared with normal-threshold cells ($P = 0.51$ for rows, $P = 0.88$ for arcs, Mann–Whitney), and Contact + Detach compared with Pressure cells ($P = 0.36$ for rows, $P = 0.75$ for arcs, Mann–Whitney).

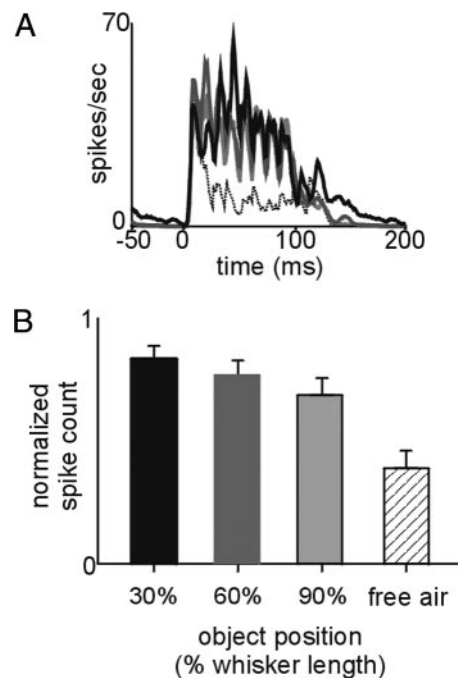


FIG. 7. Encoding of radial object position by Whisking/Touch cells. A: PSTH of the response of cells ($n = 15$) during whisking in free air (dotted line) and at objects located at 90% (light gray line), 60% (dark gray line), and 30% (black line) of the length of the whisker; 30, 60, and 90% lines are overlaid on the free-air line. B: mean spike counts per position normalized to maximum.

DISCUSSION

We showed how TG neurons encode the radial location of a vertical object. The types of responses observed did not differ qualitatively from those previously reported by Szwed et al. (2003). Division of TG neurons into Touch, Touch subtypes, Whisking/Touch, and Whisking cells was similar in both studies, revealing functionally distinct groups of first-order neurons that differ in the type of information efficiently conveyed (Tables 1 and 2, Fig. 5).

In the TG the horizontal dimension is encoded by both temporal and combined temporal-identity codes (Szwed et al. 2003). Our present findings expand the understanding of encoding of object position in the rat trigeminal system by showing how a second spatial dimension—the radial—is encoded predominantly by spike count. Thus the principal variable used to encode object location appears to differ across the horizontal and radial dimensions: timing of Contact cells for the horizontal and spike count of Touch cells for the radial coordinate. Secondary variables also carry meaningful information, which might be decoded in addition for more secure or more rapid processing. The vertical (third) dimension is probably encoded by the identity of the whisker row activated because TG receptive fields contain only one whisker and the whiskers move mostly along the rows, with little or no overlap along the vertical dimension (Bermejo et al. 2002). This conjecture, however, will have to be tested in freely moving rats.

Comparison with previous results

Classical experiments on the TG were conducted with passive stimuli applied to stationary vibrissae (Gibson and Welker 1983a; Lichtenstein et al. 1990; Shoykhet et al. 2000; Zucker and Welker 1969). Because these studies used stimuli applied to a single location at the most proximal (4–10 mm) part of the whisker, information on responses in TG to passive stimuli applied at more distal points of the whisker was lacking. In a pioneering study, Armstrong-James and Ebner (2003) applied near-threshold, passive deflections of constant amplitude at three different points along the whisker, and recorded single-unit responses from the SI somatosensory cortex. Stimuli applied 2 mm from the whisker root produced, on average, a threefold greater response than that of stimuli applied to the middle of the whisker, and a 10-fold greater response than that of stimuli applied 2 mm from the tip of the whisker. Whether passive stimuli of the same angular amplitude would produce similar results is not yet known. The passive and the active modes of whisker stimulation differ significantly (Szwed et al. 2003), mainly because the intrinsic muscle does not exert force on the follicle in the passive mode (Fig. 1, *B* and *C*). Thus a direct connection of the findings of Armstrong-James and Ebner (2003) with ours is difficult. Nonetheless, parallels between the passive and active paradigms exist. For example, during active touch higher contact velocity led to higher spike counts (Fig. 4), which is similar to TG neurons' encoding of passive stimulus velocity by increased spike counts (Arabzadeh et al. 2005; Gibson and Welker 1983b; Shoykhet et al. 2000). Furthermore, the heterogeneities we observed in response thresholds and magnitudes were similar to those observed with passive stimuli [see Figs. 1 and 11 in Gibson and Welker (1983b) and Fig. 3 in Lichtenstein et al. (1990)]. The

mechanisms generating gradual rate coding of radial distance during active touch thus might be the same mechanisms that generate gradual rate coding of amplitude and velocity during passive touch.

TG cells respond to increased stimulus velocity by firing more spikes (Arabzadeh et al. 2005; Gibson and Welker 1983a,b; Lichtenstein et al. 1990; Zucker and Welker 1969). This study confirms that the above observation is also valid for active touch. However, we found that the complex mechanical structure of the whisker makes it impossible to predict spike rate from tangential stimulus velocity alone while disregarding the radial position along the whisker at which touch occurs and that a linear combination of the effects of radial object position and whisker angular velocity at touch can explain about 73% of TG neurons' spike rate.

High-threshold cells

Locating an object at various radial positions revealed a possible role for Touch cells with high response thresholds. These neurons, which did not respond to objects touched by the distal tip of the whisker, were good detectors of proximal touch because they fired only when the object was close enough to the base of the whisker (Fig. 3, *J* and *L*). Such behavior can be interpreted as expressing a form of identity (labeled-line) code, where the presence of a spike by itself encodes information, in this case the presence of an object close to the snout. The identity code can be regarded as a particular form of a spike-count code. However, an identity code and a gradual spike-count code differ in the way they can be read out. A spike-count code is gradual and requires a transformation or comparison with other values (expected or acquired). An identity code, because of its all-or-none nature, can be simply relayed downstream, in principle even directly to a motor output. Our results therefore suggest that high-threshold Touch cells might function as proximal-touch all-or-none detectors, whereas low-threshold Touch cells encode radial position in a gradual form along the entire whisker length.

Encoding of radial distance

All 38 Touch cells examined encoded radial object location with a spike-count code. Subpopulations of Touch cells also encoded radial object by other response variables (see Table 2 and Figs. 3 and 5). First, 50% of Pressure cells encoded more proximal object positions by decreasing their ISIs. Second, Touch cells with high thresholds encoded proximal object positions by an identity code. Finally, Pressure cells encoded closer object positions by decreased delay between whisker-object contact and the first spike (Figs. 2, 3, and 5).

Spike count per cycle was the most robust code, as determined by its efficiency and the number of encoding cells (all Touch cells; Table 2). The ISI code had an efficiency similar to that of the spike-count code. However, ISI coding was possible for only half (50%) of recorded cells. The delay code was usually less efficient than the spike-count code. The information conveyed by populations of Touch neurons increased gradually with the number of participating neurons: for the spike-count code >95% average performance could already be achieved with seven cells randomly chosen from the entire Touch cell population (Fig. 6*E*).

Analysis of encoding dynamics revealed that all (100%) information about radial position carried by Contact + Detach cells and almost all (90%) information about radial position carried by Pressure cells, respectively, is already present in the first 20 ms of the response. This supports the suggestion that the continuous response of Pressure cells during protraction mainly conveys information about aspects other than location of an object, such as texture (see Arabzadeh et al. 2005), and is used to refine radial coordinates only if needed. In humans, the existence of both rapid and slow coding schemes for the same sensory variable was recently described (Johansson and Birznieks 2004). With human touch, complex features of an object are encoded by first-order neurons both in firing rate (slow code) and in relative timing of first impulses (fast code). Obviously, the mere existence of a code does not necessarily mean that it is used by an organism (Perkel and Bullock 1968); thus the potential use of various coding variables for specific tasks should be experimentally tested in behaving rats.

Possible readout mechanisms

We found that spike rate is a degenerate code because it depends both on radial position of the object and touch velocity (Fig. 4). It follows that to decode radial object position the brain should either include velocity information into the computation and/or keep the velocity constant during touch. The vibrissal system probably uses both strategies. Spike rates of SI cortex neurons correlate with whisking amplitude (Fee et al. 1997); this could provide the decoding circuit with information about whisker velocity because whisking amplitude is tightly correlated with velocity during artificial whisking (see *Artificial whisking and the experimental paradigm*) and self-evoked exploratory whisking (Knutsen et al. 2004). Also, during exploratory whisking in free air, rats maintain constant whisker velocity in the protraction phase (Knutsen et al. 2004, 2005).

Because all Touch cells encode radial object position by spike count, this code could be read out by a circuit that integrates input from any group of Touch cells. The other codes could be read out only if the putative readout mechanisms received input from the specific Touch cell subpopulation that carried the relevant information. For the delay to the first spike code and the high-threshold identity code, achieving the required specificity would probably involve selectivity in synaptic connectivity. Specificity required for reading the ISI code could also be achieved by means of highly facilitating synapses (Markram et al. 1998). Readout neurons that receive input through such synapses would respond only to Touch cells that fire more than one spike per whisking cycle (i.e., essentially only Pressure cells with spike rates ≥ 2 spikes/whisk). Facilitating synapses could also provide a way of reading out the ISI signal because pairs of spikes arriving at smaller intervals would cause larger excitatory postsynaptic potentials.

Recently, TG neurons were shown to be capable of conveying accurate temporal information (Arabzadeh et al. 2005; Jones et al. 2004b). Previously we discovered that delay from protraction onset to the first spike of Contact neurons, and to a lesser degree of Pressure neurons, can be used to encode horizontal object location (Szwed et al. 2003). Now, we report that the timing of the first spike of Pressure cells is also influenced by the radial position, whereas that of Contact cells (excluding the four "type crossing" cells) is not. Therefore first

spike timing of Pressure cells is not a reliable code for either a radial or a horizontal coordinate because it is affected by both coordinates. In contrast, the timing of the first spike of Contact cells is a reliable indicator of the horizontal coordinate of touch because it is not affected by the radial coordinate.

Behavioral implications

Brecht and colleagues (1997) analyzed the organization of the whisker array and found that whiskers from different arcs have different lengths: from 40 to 50 mm (row D) and 35 to 44 mm (row A) for the posteriormost (greek) arc, to 11–13 mm (row D) and 9–10 mm (row A) for the 4th arc. A similar gradient was reported later by Haidarliu and Ahissar (2001). Brecht et al. (1997) suggested that the rat could use this length gradient to encode radial distances of objects: the more distant an object the fewer whiskers would touch it. Such a touched/untouched signal could be decoded by simply sensing which whiskers were touched and which were untouched (see Fig. 7 in Brecht et al. 1997).

This idea was tested by Krupa et al. (2001), who trained rats to discriminate between apertures of similar size. The rats detected small (≥ 3 mm) differences in aperture size using their whiskers. Removal of more and more whiskers gradually decreased performance, and rats with no macrovibrissae performed at a chance level. However, task performance did not depend on which whiskers were removed. Moreover, with 8–12 whiskers remaining on each side, all whiskers touched the aperture walls while discriminating both narrow and wide apertures, and yet the success rate of the rats was $>75\%$. Krupa et al. (2001) concluded that "... although a binary touched/untouched signal may be sufficient to perform discriminations when the apertures are fairly different, more complex tactual information from individual whiskers must be integrated by the trigeminal system to discriminate between similar apertures." Such information could be carried by the neuronal variables described in the present report, primarily by spike counts.

In the above experiment (Krupa et al. 2001), rats did not whisk while performing the task, and whiskers were moved against the aperture walls by moving the entire rat. Thus the whisker stimulation was more similar to deflecting passive whiskers than to blocking actively moving whiskers as studied herein. Nevertheless, given the similarities between the operational variables encoding radial location during passive and active vibrissal touch (see *Comparison with previous results*), the variables described by us are expected to be relevant for radial coding in both active and passive vibrissal touch. This is probably not the case with the encoding of the horizontal coordinate, where whisker movement plays a crucial role (Szwed et al. 2003). Overall, our results suggest that during whisking the three spatial coordinates are encoded each by a separate neuronal variable: cell identity for the vertical coordinate, spike timing for the horizontal coordinate, and spike rate for the radial coordinate.

ACKNOWLEDGMENTS

We thank P. Knutsen, I. Lampl, and J. Stehberg for critically reviewing the manuscript, B. Schick for reviewing and editing, N. Rubin for programming, S. Panzeri for advice on MJ analysis, and S. Haidarliu for drawings. E. Ahissar holds the Helen Diller Family Professorial Chair of Neurobiology.

GRANTS

This work was supported by the Israel Science Foundation Grant 377/02–1, the Minerva Foundation, the Edith C. Blum Foundation, the Irving B. Harris Foundation, and the Human Frontier Science Program. K. Bagdasarian was supported by the Giladi program, Ministry of Absorption, Israel.

REFERENCES

- Arabzadeh E, Zorzin E, and Diamond ME.** Neuronal encoding of texture in the whisker sensory pathway. *PLoS Biol* 3: e17, 2005.
- Armstrong-James MA and Ebner FF.** Effect of locus and oscillation damping during whisker stimulation on the response of barrel field cortex neurons in anesthetized adult rats. *Soc Neurosci Abstr* 59.12, 2003.
- Berg RW and Kleinfeld D.** Rhythmic whisking by rat: retraction as well as protraction of the vibrissae is under active muscular control. *J Neurophysiol* 89: 104–117, 2003.
- Bermejo R, Vyas A, and Zeigler HP.** Topography of rodent whisking—I. Two-dimensional monitoring of whisker movements. *Somatosens Mot Res* 19: 341–346, 2002.
- Borst A and Theunissen FE.** Information theory and neural coding. *Nat Neurosci* 2: 947–957, 1999.
- Brecht M, Preilowski B, and Merzenich MM.** Functional architecture of the mystacial vibrissae. *Behav Brain Res* 84: 81–97, 1997.
- Britten KH, Shadlen MN, Newsome WT, and Movshon JA.** The analysis of visual motion: a comparison of neuronal and psychophysical performance. *J Neurosci* 12: 4745–4765, 1992.
- Brown AW and Waite PM.** Responses in the rat thalamus to whisker movements produced by motor nerve stimulation. *J Physiol* 238: 387–401, 1974.
- Carvell GE and Simons DJ.** Biometric analyses of vibrissal tactile discrimination in the rat. *J Neurosci* 10: 2638–2648, 1990.
- Carvell GE and Simons DJ.** Task- and subject-related differences in sensorimotor behavior during active touch. *Somatosens Mot Res* 12: 1–9, 1995.
- Dayan P and Abbott LF.** *Theoretical Neuroscience: Computational and Mathematical Modeling of Neural Systems*. Cambridge, MA: MIT Press, 2001.
- Dehnhardt G, Mauck B, Hanke W, and Bleckmann H.** Hydrodynamic trail-following in harbor seals (*Phoca vitulina*). *Science* 293: 102–104, 2001.
- Ebara S, Kumamoto K, Matsuura T, Mazurkiewicz JE, and Rice FL.** Similarities and differences in the innervation of mystacial vibrissal follicle-sinus complexes in the rat and cat: a confocal microscopic study. *J Comp Neurol* 449: 103–119, 2002.
- Fee MS, Mitra PP, and Kleinfeld D.** Central versus peripheral determinants of patterned spike activity in rat vibrissa cortex during whisking. *J Neurophysiol* 78: 1144–1149, 1997.
- Fundin BT, Arvidsson J, Aldskogius H, Johansson O, Rice SN, and Rice FL.** Comprehensive immunofluorescence and lectin binding analysis of interwhisker fur innervation in the mystacial pad of the rat. *J Comp Neurol* 385: 185–206, 1997.
- Gibson JM and Welker WI.** Quantitative studies of stimulus coding in first-order vibrissa afferents of rats. 1. Receptive-field properties and threshold distributions. *Somatosens Res* 1: 51–67, 1983a.
- Gibson JM and Welker WI.** Quantitative studies of stimulus coding in first-order vibrissa afferents of rats. 2. Adaptation and coding of stimulus parameters. *Somatosens Res* 1: 95–117, 1983b.
- Gottschaldt KM, Iggo A, and Young DW.** Functional characteristics of mechanoreceptors in sinus hair follicles of the cat. *J Physiol* 235: 287–315, 1973.
- Gottschaldt KM and Vahle-Hinz C.** Merkel cell receptors: structure and transducer function. *Science* 214: 183–186, 1981.
- Green DM and Swets JA.** *Signal Detection Theory and Psychophysics*. New York: Wiley, 1966.
- Haidarliu S and Ahissar E.** Size gradients of barreloids in the rat thalamus. *J Comp Neurol* 429: 372–387, 2001 (Erratum. *J Comp Neurol* 431: 127–128, 2001).
- Hartmann MJ, Johnson NJ, Towal RB, and Assad C.** Mechanical characteristics of rat vibrissae: resonant frequencies and damping in isolated whiskers and in the awake behaving animal. *J Neurosci* 23: 6510–6519, 2003.
- Hutson KA and Masterton RB.** The sensory contribution of a single vibrissa's cortical barrel. *J Neurophysiol* 56: 1196–1223, 1986.
- Jacquin MF, Golden J, and Rhoades RW.** Structure–function relationships in rat brainstem subnucleus interparietalis: III. Local circuit neurons. *J Comp Neurol* 282: 24–44, 1989.
- Jenkinson EW and Glickstein M.** Whiskers, barrels, and cortical efferent pathways in gap crossing by rats. *J Neurophysiol* 84: 1781–1789, 2000.
- Johansson RS and Birznieks I.** First spikes in ensembles of human tactile afferents code complex spatial fingertip events. *Nat Neurosci* 7: 170–178, 2004.
- Jones LM, Depireux DA, Simons DJ, and Keller A.** Robust temporal coding in the trigeminal system. *Science* 304: 1989–1993, 2004a.
- Jones LM, Lee S, Trageser JC, Simons DJ, and Keller A.** Precise temporal responses in whisker trigeminal neurons. *J Neurophysiol* 92: 665–668, 2004b.
- Knutsen PM, Derdikman D, and Ahissar E.** Tracking whisker and head movements in unrestrained behaving rodents. *J Neurophysiol* 93: 2294–2301, 2005.
- Knutsen PM, Pietr M, and Ahissar E.** Trajectory control during rodent whisking. Proceedings of the 13th Annual Meeting of the Israel Society for Neuroscience, Eilat, Israel. *Neural Plast* 12: 32, 2004.
- Krupa DJ, Matell MS, Brisben AJ, Oliveira LM, and Nicolelis MA.** Behavioral properties of the trigeminal somatosensory system in rats performing whisker-dependent tactile discriminations. *J Neurosci* 21: 5752–5763, 2001.
- Krupa DJ, Wiest MC, Shuler MG, Laubach M, and Nicolelis MA.** Layer-specific somatosensory cortical activation during active tactile discrimination. *Science* 304: 1989–1992, 2004.
- Lichtenstein SH, Carvell GE, and Simons DJ.** Responses of rat trigeminal ganglion neurons to movements of vibrissae in different directions. *Somatosens Mot Res* 7: 47–65, 1990.
- Lo FS, Guido W, and Erzurumlu RS.** Electrophysiological properties and synaptic responses of cells in the trigeminal principal sensory nucleus of postnatal rats. *J Neurophysiol* 82: 2765–2775, 1999.
- Markram H, Gupta A, Uziel A, Wang Y, and Tsodyks M.** Information processing with frequency-dependent synaptic connections. *Neurobiol Learn Mem* 70: 101–112, 1998.
- Morrison DF.** *Multivariate Statistical Methods* (2nd ed.). New York: McGraw-Hill, 1976.
- Nguyen KT and Kleinfeld D.** Positive feedback in a brainstem tactile sensorimotor loop. *Neuron* 45: 447–457, 2005.
- Neimark MA, Andermann ML, Hopfield JJ, and Moore CI.** Vibrissa resonance as a transduction mechanism for tactile encoding. *J Neurosci* 23: 6499–6509, 2003.
- Panzeri S and Schultz SR.** A unified approach to the study of temporal, correlational, and rate coding. *Neural Comp* 13: 1311–1349, 2001.
- Panzeri S and Treves A.** Analytical estimates of limited sampling biases in different information measures. *Network* 7: 87–107, 1996.
- Perkel DH and Bullock TH.** Neural coding. *Neurosci Res Program Bull* 6: 221–248, 1968.
- Rice FL, Mance A, and Munger BL.** A comparative light microscopic analysis of the sensory innervation of the mystacial pad. I. Innervation of vibrissal follicle-sinus complexes. *J Comp Neurol* 252: 154–174, 1986.
- Sachdev RN, Egl M, Stonecypher M, Wiley RG, and Ebner FF.** Enhancement of cortical plasticity by behavioral training in acetylcholine-depleted adult rats. *J Neurophysiol* 84: 1971–1981, 2000.
- Schneider JS, Denaro FJ, Olazabal UE, and Leard HO.** Stereotaxic atlas of the trigeminal ganglion in rat, cat, and monkey. *Brain Res Bull* 7: 93–95, 1981.
- Semba K and Egger MD.** The facial “motor” nerve of the rat: control of vibrissal movement and examination of motor and sensory components. *J Comp Neurol* 247: 144–158, 1986.
- Shannon CE.** A mathematical theory of communication. *Bell System Tech J* 27: 379–423, 623–656, 1948.
- Shoykhet M, Doherty D, and Simons DJ.** Coding of deflection velocity and amplitude by whisker primary afferent neurons: implications for higher level processing. *Somatosens Mot Res* 17: 171–180, 2000.
- Sosnik R, Haidarliu S, and Ahissar E.** Temporal frequency of whisker movement. I. Representations in brain stem and thalamus. *J Neurophysiol* 86: 339–353, 2001.
- Szved M, Bagdasarian K, and Ahissar E.** Encoding of vibrissal active touch. *Neuron* 40: 621–630, 2003.
- Tracey DJ and Waite PME.** Somatosensory system. In: *The Rat Nervous System*, edited by Paxinos G. San Diego, CA: Academic Press, 1995, p. 689–704.
- Vincent SB.** The function of the vibrissae in the behavior of the white rat. *Behav Monogr* 1: 7–81, 1912.
- Welker WI.** Analysis of sniffing of the albino rat. *Behaviour* 12: 223–244, 1964.
- Zucker E and Welker WI.** Coding of somatic sensory input by vibrissae neurons in the rat's trigeminal ganglion. *Brain Res* 12: 138–156, 1969.